Far infrared reflectivity spectra of lead-telluride doped with Mn and Yb

P. M. NIKOLIC[*], K. M. PARASKEVOPOULOS[a], T. T. ZORBA[a], Z. Z. DJURIC, E. PAVLIDOU[a], S. S. VUJATOVIC, V. BLAGOJEVIC[c], O. S. ALEKSIC[b], M. V. NIKOLIC[b]
Institute of Technical Sciences of SASA, Knez Mihailova 35/IV, 11000 Belgrade, Serbia
[a]*Physics Department, Solid State Section, Aristotle University of Thessaloniki, 54124 Thessaloniki, Greece*
[b]*Institute for Multidisciplinary Research, University of Belgrade, Kneza Viseslava 1, 11000 Beograd, Serbia*
[c]*Faculty of Electrical Engineering, University of Belgrade, Bulevar Kralja Aleksandra 73, 11000 Belgrade, Serbia*

PbTe single crystal samples doped with Mn and Yb were grown using the Bridgman method. Far infrared reflectivity spectra were measured at room temperature for samples with different impurity concentrations (total impurity concentration Mn+Yb varied between 0.59 and 2.52 at%, while the impurity Mn/Yb ratio varied between 0 and 3.48). All samples were of the "p" type. Plasma minimum was registered for all samples and varied between 114 and 198 cm^{-1} depending on the total impurity concentration and ratio. Samples with lower plasma minimum had a higher free hole mobility, with the highest value of 7000 cm^2/Vs determined for a sample with the highest Mn/Yb ratio of 3.48 (1.67 at.% Mn and 0.48 at.% Yb).

(Received August 21, 2012; accepted June 12, 2013)

Keywords: Semiconductors, Lead telluride, Far infrared reflectivity, Dopants

1. Introduction

Modification of properties of narrow-gap IV-VI semiconductors by doping with various impurities remains in focus as the presence of impurity states gives rise to a number of unique properties [1]. These properties depend not only on the impurity used, but also the impurity content. Doping with group III impurities, such as In, Ga or Tl leads to new effects such as Fermi level pinning and persistent photoconductivity at low temperatures [2]. Transition metals also act as either donors (Cr, Co, Ni, Ti) or neutrals (Mn) [1]. Similar impurity states were also observed in PbTe doped with Cr [3] where the Fermi level becomes pinned in the conduction band.

In the case of Yb, Skipetrov et al [4] performed detailed electric and magnetic characterization of $Pb_{1-y}Yb_yTe$ semiconductors and determined that ytterbrium also modifies the energy spectrum of charge carriers in PbTe by formation of deep impurity levels. At low Yb content this deep level is resonant with the valence band, while with increasing impurity concentration it approaches the valence band edge and shifts into the forbidden band. The ytterbium ion is present in $Pb_{1-y}Yb_yTe$ in two charge states. The first is magnetically active Yb^{3+}, whose concentration increases with increase in Yb content and constitutes about 10-15% of total Yb content. The second are non-magnetic Yb^{2+} ions. Mixed valence of Yb was confirmed in analysis of far infrared spectra [5]. EPR measurements have shown that Yb^{3+} ion substitutes for the Pb^{2+} ions in PbS, PbSe and PbTe [6]. For a uniformly doped PbTe+Yb crystal with 1.3 at% Yb, X-ray Absorption Fine Structure (XAFS) at room temperature and 20K have been measured [7]. Analysis of the near edge (XANES) region also revealed mixed-valence behavior of Yb. It was concluded that at 20K the mean valence of Yb is 2.12+ (12% Yb^{3+}) and it is slightly larger at room temperature (2.16+, 16% Yb^{3+}). The high energy region of the absorption spectra (EXAFS) revealed that Yb addition causes extension of nearest neighbor distances around all atoms in that compound, which is more pronounced around the Yb impurity.

Thus, IV-VI narrow-gap semiconductors doped with magnetic impurities of variable-mixed valence such as Yb, Gd, Eu, Cr or Mn are known as diluted magnetic semiconductors where magnetic properties strongly depend on their electronic structure e.g. energy position of the deep impurity level relative to the band edges and occupancy of that level with electrons [8]. In the case of the $Pb_{1-x}Mn_xTe$ solid solution, if the Mn concentration is less than 20 at.%, Mn enters the PbTe lattice as Mn^{2+} and is not an electroactive dopant. Doping with Mn increases the bandgap, but no local or quasilocal levels appear in the vicinity of the actual bands [9]. The behavior of $Pb_{1-x}Mn_xTe$ with a substantial magnetic signal in the specific heat was observed below 1K [10]. More recently single crystals of $Pb_{1-x}Mn_xTe$ were studied [11] including their transport and magnetic properties [12].

Simultaneous doping of PbTe has resulted in further interesting effects. The giant negative magnetoresistance effect was observed in PbTe doped simultaneously with Yb and Mn [13]. For some impurity concentrations the sample resistance dropped about three values of magnitude when the magnetic field increased up to 5-6 T. In this case this effect is the result of a combined action of both dopants and depends on their concentrations and the impurity concentration ratio. Only samples with Yb

concentration high enough to provide the Fermi-level pinning effect were analyzed (0.54 at%-1.03 at%) in [13], while the Mn content varied between 2.01 and 2.39 at%, making the Mn/Yb ratio in the range between 4.42 and 1.95. A much lower magnitude of negative magnetoresistance was observed in PbTe doped simultaneously with Mn and Cr [3], while Yb doped $Pb_{1-x}Ge_xTe$ does not exhibit giant negative magnetoresistance [14]. Obviously the giant negative magnetoresistance effect is the result of the interaction between Mn and Yb impurities. Some possible explanations were given by Ivanchik et al [13], but further research is needed to clarify its origin.

In this work we have analyzed far infrared reflectivity spectra of lead telluride co-doped with Mn and Yb. Our purpose was to analyze how different impurity content and their ratio influenced optical properties. We focused on changes of the plasma frequency and room temperature free carrier optical mobility.

2. Experimental

Two single crystals of PbTe doped with Mn and Yb were produced using the Bridgman technique as described in [15]. The first had a starting composition of 4 at% Mn and 1 at% Yb while the second ingot had 0.5 at% Mn and 2 at% Yb. High purity elements (6N) were used as the source material. As the dopant concentration varied along the growth axis, samples with different dopant concentrations between 1 and 2 mm thick were cut or cleaved perpendicular to the *c* axis from the produced crystals. X-ray diffraction measurements on a Philips PW 1050 diffractometer proved that the obtained crystal ingots were single crystals, which could be cleaved perpendicular to the *c* axis. The content of Pb, Te, Mn and Yb in each sample was determined using EDS analysis. Far infrared reflectivity spectra were measured at room temperature using a Bruker IFS-113 V spectrometer.

3. Results and discussion

Far infrared reflectivity spectra of Mn and Yb doped PbTe single crystal samples are given in Fig. 1. Four diagrams for samples where the percentage of Mn was above 1 at% and Yb less than 0.73 at% are given in Fig. 1a. Three of these samples had a plasma minimum at about 115 cm^{-1} and one at about 120 cm^{-1}. Fig. 1b shows three reflectivity spectra of samples with a larger percentage of Yb (samples 5 and 6). In sample 7 it is the only dopant. For these three samples where the percentage of Mn is between $0 \leq Mn < 0.34$ at% and of Yb, between $0.25 < Yb < 1.6$ at%, the plasma minimum is at much higher wave numbers, between 182 and 192 cm^{-1}. Exact atomic percentages of elements determined by EDS analysis in each sample are given in Table 1. The first four (1-4) samples were cut from the first ingot and the next three samples (5-7), from the second ingot.

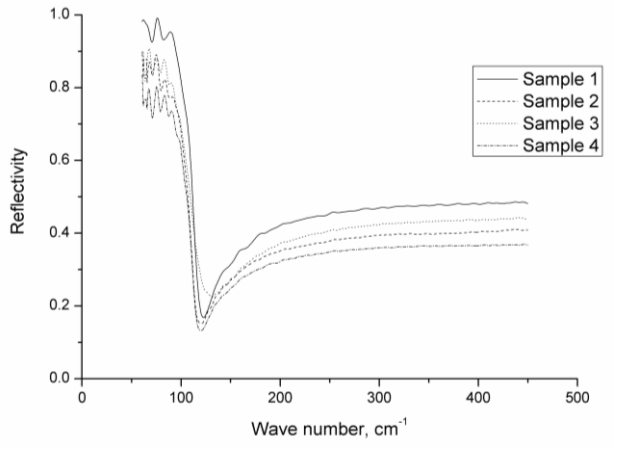

a

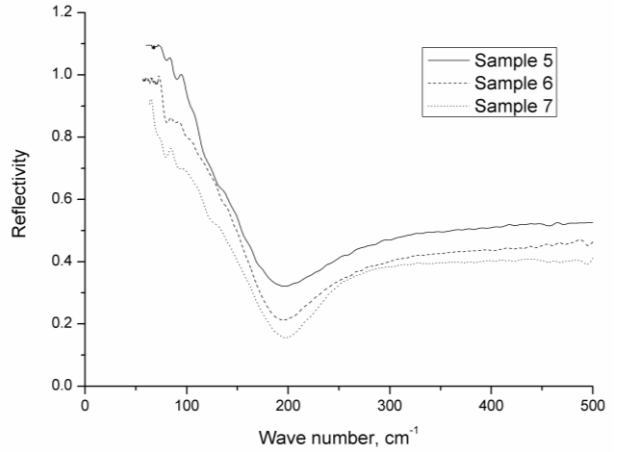

b

Fig. 1. Room temperature FIR diagrams for (a) samples (1-4): 1) $Pb_{0.4614}Mn_{0.0167}Yb_{0.0048}Te_{0.517}$; 2) $Pb_{0.465}Mn_{0.0179}Yb_{0.0073}Te_{0.5096}$; 3) $Pb_{0.464}Mn_{0.0121}Yb_{0.0053}Te_{0.5184}$; 4) $Pb_{0.4911}Mn_{0.0117}Yb_{0.0068}Te_{0.4913}$; (b) samples (5-7): 5) $Pb_{0.461}Mn_{0.0034}Yb_{0.0025}Te_{0.533}$; 6) $Pb_{0.46}Mn_{0.0015}Yb_{0.0095}Te_{0.528}$; 7) $Pb_{0.466}Yb_{0.016}Te_{0.517}$.

Table 1. Calculated parameters for PbTe doped with Mn and Yb.

PbTe+Mn+Yb	at%	ω_p (cm^{-1})	γ_p (cm^{-1})	ε_α	R_{min}	μ_p (cm^2/Vs)	p (cm^{-3}) $\times 10^{-18}$	at% (Mn/Yb)
Sample1	Yb=0.48;Mn=1.67 Pb=46.14;Te=51.7	117	13.5	30.0	0.157	7031	0.728	3.48
Sample2	Yb=0.73;Mn=1.79 Pb=46.5;Te=50.96	~114	16.8	26.2	0.150	4938.5	0.741	2.45
Sample3	Yb=0.53;Mn=1.21 Pb=46.4;Te=51.84	114.6	14.0	26.1	0.140	4283	0.727	2.28
Sample4	Yb=0.68;Mn=1.17 Pb=49.11;Te=49.13	119.2	24.8	26.0	0.226	2495.5	0.775	1.72
Sample5	Yb=0.25;Mn=0.34 Pb=46.1;Te=53.3	184	68.8	38.9	0.320	870	2.54	1.36
Sample6	Yb=0.95;Mn=0.15 Pb=46.0;Te=52.8	182	54.2	37.4	0.220	1950	2.51	0.15
Sample7	Yb=1.6;Mn=0 Pb=46.6;Te=51.7	192.8	49.0	28.7	0.140	2182	2.90	0

The measured experimental diagrams were numerically analyzed using a modified four parameter model of coupled oscillators first introduced by Gervais and Piriou [16]. In this case the dielectric function takes into account the existence of a plasmon-phonon interaction, i.e. the pure longitudinal –LO modes of the lattice are strongly influenced by the plasma mode of free carriers [17]. The conventional two-oscillator dielectric function using the Drude model together with a lattice term has often been applied to analyze reflectivity of PbTe [18]. However, in PbTe-based systems the pure longitudinal LO-modes of the lattice are strongly influenced by the plasmon mode of free carriers, so combined plasmon-LO phonon modes were observed. In experimental spectra only coupled mode positions could be noted [19], so determination of LO modes included elimination of the influence of free carriers [5, 17, 19, 20] as follows:

$$\varepsilon(\omega)=\varepsilon_\infty\frac{\prod_{j=1}^{2}(\omega^2+\gamma_{lj}\omega-\omega_{lj}^2)}{\omega(\omega+i\gamma_p)(\omega^2+i\gamma_t\omega-\omega_t^2)}\prod_{n=1}^{p}\frac{\omega^2+i\gamma_{Ln}\omega-\omega_{Ln}^2}{\omega^2+i\gamma_{0n}\omega-\omega_{0n}^2}\prod_{k=1}^{q}\frac{\omega^2+i\gamma_{LOk}\omega-\omega_{LOk}^2}{\omega^2+i\gamma_{TOk}\omega-\omega_{TOk}^2} \quad (1)$$

where ω_{lj} and γ_{lj} are parameters of the first numerator representing eigenfrequencies and damping factor of the plasmon-LO phonon waves, respectively. First denominator parameters correspond to similar characteristics of the transverse vibrations. γ_p is the plasmon mode damping factor and ε_∞ represents the high frequency dielectric permittivity relative to the spectral interval of interest. The second term represents local impurity modes, while in the third term ω_{LOk}, ω_{TOk}, γ_{LOk} and γ_{TOk} represent longitudinal and transverse frequencies and damping factors of the host crystal uncoupled modes. This model has been used to analyze far infrared reflectivity spectra of PbTe doped with Yb [5], Mn [19,20] and other dopants [21,22].

All parameters of the applied model can be fitted separately or together and the user can select the magnitude of change of each parameter. The starting values of all parameters used in the fitting procedure were previously calculated using Kramers-Kronig analysis [23]. As the reflectivity spectra were measured down to 50 cm^{-1}, the value for the transverse phonon frequency, ω_t was taken from literature to be 32 cm^{-1} [21,22]. The plasma frequency was determined using the extended Lyddane-Sachs-Teller (LST) relation introduced by Kukharskii [17]: $\omega_p = \omega_{l1}\cdot\omega_{l2}/\omega_t$.

Fig. 2a and 2b show room temperature reflectivity diagrams for samples 1 and 5. Experimental spectrums are presented by circles while the solid lines represent calculated values. Good agreement between experimental and calculated data can be noted. The frequencies determined for the two coupled modes (ω_{l1} and ω_{l2}) were used to calculate the plasma frequency ω_p. The weak oscillator at about 70 cm^{-1} belongs to the edge of the Brillouin zone as the phonon density of PbTe has a maximum at these frequencies. Such oscillators were noted for PbTe doped with Yb [5] and Mn [19,20]. The mode at 105 cm^{-1} represents the LO mode of pure PbTe [5].

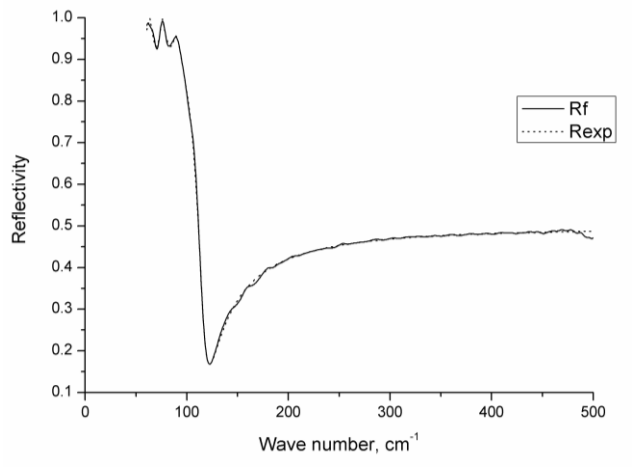

a

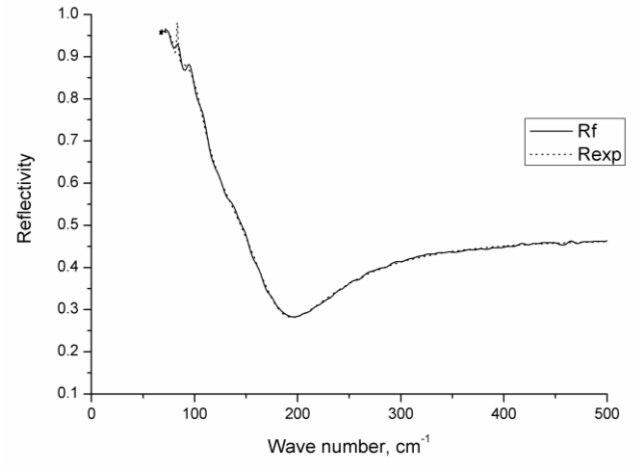

b

Fig. 2. Far infrared reflectivity spectrum of (a) $Pb_{0.4614}Mn_{0.0167}Yb_{0.0048}Te_{0.517}$ (b) $Pb_{0.461}Mn_{0.0034}Yb_{0.0025}Te_{0.533}$. Experimental spectrum is presented by points while the full line was calculated using the fitting procedure.

The values of the main calculated optical and electrical parameters of the samples presented in Fig. 1a and Fig. 1b are given in Table 1. They are: ω_p- plasma frequency; its damping factor- γ_p; ε_∞- the high frequency relative to the spectral interval of interest; R_{min}- optical reflectivity coefficient at plasma frequency. The optical mobility of free carriers (μ_p) was calculated using the method of Moss et al [24]. The technique of studying plasma edge reflectivity to provide relatively accurate data on free carrier concentrations developed by Moss et al [24] was also used to calculate the majority free carrier (hole) concentration (p) and these results are also given in Table 1. Analysis of the data given in Table 1 shows that, lower values of plasma frequency were obtained for samples with a higher Mn/Yb ratio and overall dopant content. The Yb content ranged between 0.48 and 0.73 at%, while the Mn content ranged between 1.17 and 1.79, resulting in the Mn/Yb ratio ranging between 1.72 and 3.48, with the overall dopant content in the range 1.74 to 2.52 at%. The plasma frequency was higher in samples with lower Mn content and lower Mn/Yb ratio, even though the Yb content varied between 0.25 and 1.6 at%. It is also interesting to observe changes in the optical mobility of free carriers. The highest value was obtained in the sample with the highest Mn/Yb ratio. Higher values were obtained in samples with a lower plasma frequency, higher Mn/Yb ratio and overall dopant content. The lowest value of the optical mobility of free carriers was obtained for the sample with the lowest overall dopant content. The majority free carrier (hole) concentration was lower for samples with lower plasma frequency (first ingot), while for the second ingot with higher values of plasma frequency p was higher. Obviously the amount of each dopant and their relative ratio has a significant influence on the optical properties and also overall physical properties in accordance with Ivanchik et al [13].

Far infrared reflectivity spectra of PbTe doped with Yb [5] and Mn [19,20] were analyzed for different dopant content in the temperature range 10-300K enabling determination of the origin of all oscillators present. In this work we have analyzed room temperature infrared reflectivity spectra, obviously measurements at lower temperatures could possibly give more clear information on the modes, especially impurity modes, present in the spectra.

In the case of PbTe doped with Yb two local impurity modes of Yb were observed at about 160 and 250 cm^{-1} denoting impurity atoms in different valence states [5]. The plasma frequency for PbTe doped with 0.5 at% was at about 170 cm^{-1}, while it decreased to 120 cm^{-1} for PbTe with 0.22 at%, revealing much more clearly the local impurity mode of Yb^{2+}.

In the case of PbTe doped with Mn, intermedial and two mode behaviour of long wavelength optical phonons is present, depending on the local structure of MnTe [20]. If solid solutions $Pb_{1-x}Mn_xTe$ are formed with MnTe in a cubic structure, the impurity mode of Mn is formed at about 190 cm^{-1}, but if MnTe has an orthorhombic structure the impurity mode will be formed at about 52 cm^{-1}. The plasma frequency of PbTe doped with Mn decreased with increasing dopant amount, with 228.9 determined for 0.001 at% Mn and 162 for 0.2 at% Mn [19].

It is obvious that optical properties of PbTe doped with Mn and Yb, depend greatly on the dopant amounts and their ratio. Yb deep impurity levels were determined rather close to the valence level band top, d states of Mn may affect Yb impurity states [2]. Lower plasma frequency and higher free carrier optical mobility were obtained for samples with at% Mn above 1 and higher Mn/Yb ratio and this could be expected as in PbTe doped with Yb the plasma frequency decreased with decreasing Yb content, while in PbTe doped with Mn the plasma frequency decreased with increasing Mn content.

4. Conclusion

In this work $Pb_{1-x-y}Mn_xYb_yTe$ single crystal ingots were synthesized using the Bridgman method and their far infrared optical reflectivity properties were measured and numerically analyzed using a modified four parameter model of coupled oscillators. The determined plasma frequency and free hole mobility depended on the amounts of Mn and Yb and their ratio. The lowest plasma frequency was obtained for a PbTe sample with 1.67 at% Mn and 0.48 at% Yb (highest dopant ratio of 3.48) and its free hole mobility was calculated to be above 7000 cm^2/Vs, about nine times higher than for high quality "p" type pure PbTe. This is in agreement with the impurity level model where an impurity establishes a localized state that overlaps either with the conduction or valence band of PbTe. Further work is focused on determining the optimal dopant concentration and ratio, including reflectivity measurements at low temperatures in order to further elucidate how Yb and Mn doping influences the optical properties and electronic structure of PbTe.

Acknowledgement

This work was performed as part of projects III45007 and III45014 financed by the Ministry for Science, Education and Technological Development of the Republic of Serbia.

References

[1] D. R. Khokhlov, I. I. Ivanchik, A. E. Kozhanov, A. V. Morozov, E. I. Slyn'ko, V. E. Slyn'ko, W. D. Dobrowolski, T. Story, Int. J. Mod. Phys. B **16**, 3343 (2002).
[2] B. A. Volkov, L. I. Ryabova, D. R. Khokhlov, Physics - Uspekhi **45**(8), 819 (2002).
[3] A. V. Morozov, A. E. Kozhanov, A. I. Artamkin, E. I. Slyn'ko, V. E. Slyn'ko, W. D. Dobrowolski, T. Story, D. R. Khokhlov, Semiconductors **38,** 27 (2004).
[4] E. P. Skipetrov, N. A. Chernova, L. A. Skipetrova, E. I. Slyn'ko, Mat. Sci. Eng. B **91-92**, 412 (2002).
[5] P. M. Nikolic, D. Lukovic, S. S. Vujatovic, K. Paraskevopoulos, M. V. Nikolic, V. Blagojevic, T. T. Zorba, B. Stamenovic, W. König, J. Alloy. Comp. **466**, 319 (2008).
[6] S. Isber, S. Charar, X. Gratens, C. Fau, M. Averous, S. K. Misra, Z. Golacki, Phys. Rev. B **54**, 7634 (1996).
[7] I. Radisavljevic, N. Novakovic, N. Romčevic, M. Manasijevic, H.-E. Mahnke, N. Ivanovic, J. Alloy. Comp. **501**, 159 (2010).
[8] E. P. Skipetrov, M. G. Mikheev, F. A. Pakpour, L. A. Skipetrova, N. A. Pichugin, E. I. Slyn'ko, V. E. Slyn'ko Semiconductors **43**, 297 (2009).
[9] J. Newodniczanska-Zawadzka, G. Elsinger, L. Palmetshofer, A. Lopez-Otero, E. J. Fautner, G. Bauer, W. Zawadzki, Physica B+C **117-118**, 458 (1983).
[10] A. Lusakowski, A. Jedrzejczak, M. Górska, V. Osinniy, M. Arciszewska, W. Dobrowolski, V. Domukhovski, B. Witkowska, T. Story, R. R. Gałazka, Phys. Rev. B **65**, 165206 (2002).
[11] A. V. Golubovic, S. N. Nikolic, S. Djuric, N. Z. Romcevic, J. Serb. Chem. Soc **69**, 1121 (2004).
[12] A. I. Artamkin, A. E. Kozhanov, M. Arciszewska, W. D. Dobrowolsky, T. Story, E. I. Slyn'ko, V. E. Slyn'ko, D. R. Khokhlov, Acta. Phys. Pol. A **106**, 223 (2004).
[13] I. I. Ivanchik, D. R. Khokhlov, A. V. Morozov, A. A. Terekhov, E. I. Slyn'ko, V. I. Slyn'ko, A. de Visser, W. D. Dobrowolski, Phys. Rev. B **61,** R14889 (2000).
[14] E. P. Skipetrov, N. A. Chernova, E. I. Slyn'ko, Phys. Rev. B **66**, 085204 (2002).
[15] B. A. Akimov, L. I. Ryabova, S. M. Chudinov, O. B. Yalsenko, Fiz. Tekh. Poluprov. **13**, 752 (1979).
[16] F. Gervais, B. Piriou, Phys. Rev. B **10**, 1642 (1974).
[17] A. A. Kukharskii, Solid State Commun. **13**, 1761 (1973).
[18] S. Perkowitz, Phys. Rev. B **12**, 3210 (1975).
[19] J. Trajic, M. Romcevic, N. Romcevic, S. Nikolic, A. Golubovic, S. Djuric, V. N. Nikiforov, J. Alloy. Comp. **365**, 89 (2004).
[20] J. Trajic, M. Romcevic, N. Romcevic, V. N. Nikiforov, Mater. Res. Bull. **42**, 2192 (2007).
[21] P. M. Nikolic, W. König, D. Lukovic, S. Savic, K. Radulovic, V. Blagojevic, J. Optoelectron. Adv. Mater. **6**, 811 (2004).
[22] P. M. Nikolic, K. M. Paraskevopoulos, G. Zachariadis, O. Valasiadis, T. T. Zorba, S. S. Vujatovic, N. Nikolic, O. S. Aleksic, T. Ivetic, O. Cvetkovic, V. Blagojevic, M. V. Nikolic, Optoelectron. Adv. Mater. – Rapid Commun. **6,** 2384 (2012).
[23] D. M. Roessler, Br. J. Appl. Phys. **16** 1359 (1965).
[24] T. S. Moss, T. D. F. Howkins, G. J. Burrell, J. Phys. C: Solid State Phys. **1**, 1435 (1968).

*Corresponding author: Pantelija.Nikolic@sanu.ac.rs